

Design, fabrication, and preliminary characterization of a novel MEMS bionic vector hydrophone

Chenyang Xue^b, Shang Chen^{a,b,*}, Wendong Zhang^{a,b}, Binzhen Zhang^a,
Guojun Zhang^a, Hui Qiao^a

^aNational Key Laboratory for Electronic Measurement Technology, North University of China, Taiyuan, Shanxi 030051, China

^bKey Laboratory of Instrumentation Science and Dynamic Measurement, Ministry of Education, North University of China, Taiyuan, Shanxi 030051, China

Received 11 June 2007; accepted 1 September 2007

Available online 23 October 2007

Abstract

According to the auditory principle of fish's lateral line organ, a novel microelectromechanical systems (MEMS) bionic vector hydrophone used for obtaining vector information of underwater sound field is introduced in this paper. It is desirable that the application of MEMS-based piezoresistive effect and bionics structure may improve the low-frequency sensitivity of the vector hydrophone as well as its miniaturization. The bionic structure consists of two parts: high-precision four-beam microstructure and rigid plastic cylinder which is fixed at the center of the microstructure. The piezoresistor located at the beam is simulated to the hair cell of lateral line and the rigid plastic cylinder is simulated to stereocilia. When the plastic cylinder is stimulated by sound, the piezoresistor transforms the resultant strain into a differential voltage output signal via the Wheatstone bridge circuit. Microfabrication technology has been employed for the fabrication of the microstructure and measurement results are given. The experiment results show that the receiving sensitivity of the hydrophone is -197.7 dB (0 dB = 1 V/ μ Pa). The novel hydrophone not only possesses satisfactory directional pattern as well as miniature structure, but also has good low-frequency characteristics, and satisfies the requirements for low-frequency acoustic measurement.

© 2007 Elsevier Ltd. All rights reserved.

Keywords: MEMS; Bionic; Vector hydrophone; Low frequency

1. Introduction

In underwater acoustics, the application of vector hydrophone endows several advantages for detection of submarines: It can obtain both the sound pressure and particle velocity of sound field simultaneously, effectively reduce received intensity of isotropic hindrance, and so on. Therefore, all countries with noticeable navy force have drawn unprecedented attention on the vector hydrophone and many works have been done about it. Although great achievements have been made, there are still some limitations in low-frequency detection, miniaturization, and high sensitivity.

The miniaturization of mechanical systems offers unique opportunities for scientific and technological progress, and will almost certainly open an entirely new industry [1]. Microelectromechanical systems (MEMS) refer to microscopic devices that have a characteristic length of less than 1 mm but more than 100 nm and combine electrical and mechanical components [2]. MEMS devices and systems are inherently smaller, lighter, more reliable, and faster than their macroscopic counterparts, and are usually more precise [1]. The small dimensions of microcantilevers make them excellent sensors for very sensitive detection of many physical, chemical, and biological phenomena, including acoustic signals [3–5].

Engineers, designers and architects often look to nature for inspiration. Biology has perfected its designs and formed many fruitful abilities such as its exquisite sensitivity, effectiveness, and reliability, through billions of years of evolution. So mimicking its creations is a sure

*Corresponding author. Department of Electronic Science and Technology, North University of China, Taiyuan, Shanxi 030051, China.
Tel.: +86 351 3921756; fax: +86 351 3922131.

E-mail address: csuu@sohu.com (S. Chen).

way of producing new technologies and new achievement that are both efficient and reliable [6].

The advantage of piezoresistive effect is that it can be used to detect low-frequency signal even at 0 Hz. Therefore, it is of great advantage for research on vector hydrophone based on piezoresistive effect. In this paper, a novel MEMS vector hydrophone based on the theory of bionics and piezoresistive effect will be presented, with respect to the design, fabrication, and preliminary characterization. The targeted application region for these sensors is low-frequency detection of submarine sound.

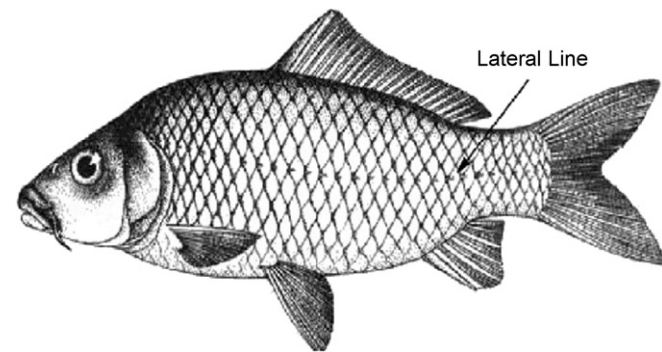


Fig. 1. Lateral line of the fish.

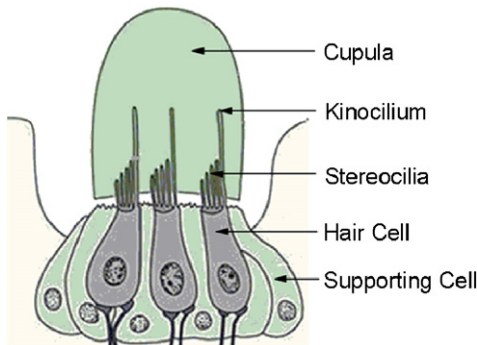


Fig. 2. Schematic view of fish's neuromast organ.

2. Basic principle

2.1. Bionics principle

An extraordinary but lesser known sensory system is the mechanosensory lateral line organ that enables the detection of minute water movements in the immediate environment [7]. The lateral line runs from the head to the tail of the fish and resembles a towed array with sensing organs (stitches) spaced at intervals along the nerve fiber (Fig. 1). Each stitch contains several neuromasts. Each neuromast comprises up to several hundred mechanosensory hair cells, more or less separated by supporting cells, and surrounding mantle cells. The apical part of the hair cell presents its stereocilia (mechanoreceptor structure) and kinocilium to the outside environment through the gelatinous cupula that covers the neuromast and makes contact with water [8,9]. Fig. 2 is the schematic view of the neuromast.

The stereocilia vibrate and act as sensors for flow noise as the fish swims through water. When stimulated by turbulence, the motion of the hair cell produces changes in the synapses which are in turn connected to the nerve fiber. The electric signal originates from impedance changes in cell walls which modulate the flow of K^+ ions. The lateral line is especially sensitive to low frequency fluid motion parallel to the length of the fish. Sound, especially low-frequency sound, travels faster and farther than in air. “Near-field” sound consists of small fluid motions or vibrations and are characterized by a displacement direction. They are detected by the inner ear or by the lateral line [10].

2.2. Acoustics theory of cylinder

Acoustics theory research indicates that for an acoustically small cylinder immersed in fluid when the size of the acoustics cylinder is far smaller than the length of sound wave, under the action of sound wave, the relation of the velocity between the cylinder and the

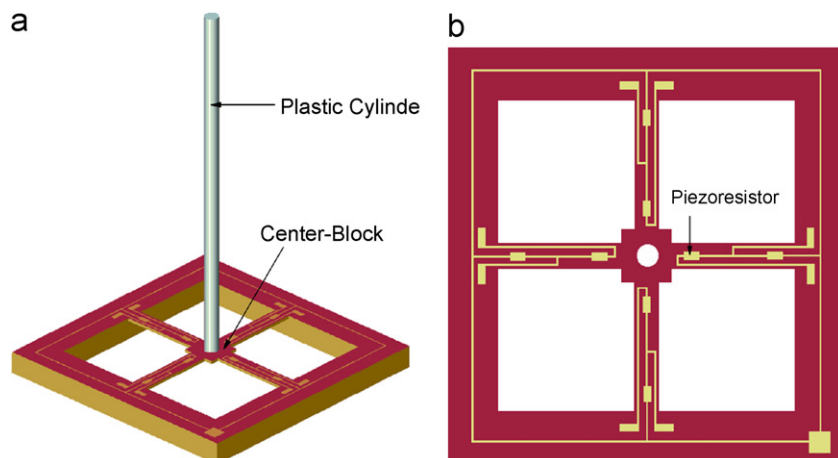


Fig. 3. (a) 3D model and (b) 2D top view of the hydrophone structure.

fluid particle is

$$\frac{V}{V_0} = \frac{4}{2 \frac{\rho}{\rho_0} + \left[\frac{\pi(ka)^2}{2} + 2j \right]}, \quad (1)$$

where V is the amplitude of the cylinder velocity, V_0 the amplitude of the particle velocity, ρ_0 the density of the fluid, ρ the density of cylinder, $k = w/c$ the wave number, and a the crustaceous radius of the cylinder. When $ka \ll 1$

$$V = \frac{2\rho_0}{\rho_0 + \rho} V_0. \quad (2)$$

This shows that at low frequencies the motion of a cylinder whose density is equal to that of the fluid it displaces is identical to the motion of the fluid particles at this location when the cylinder is removed [11–13]. Consequently, if the cylinder is fixed on an inertial transducer, a signal is produced and can be related to the acoustic particle motion.

3. Design

According to the auditory principle of lateral line organ, we can see that the mechanoreceptor structure is the stereocilia which acts as sensors for flow noise by

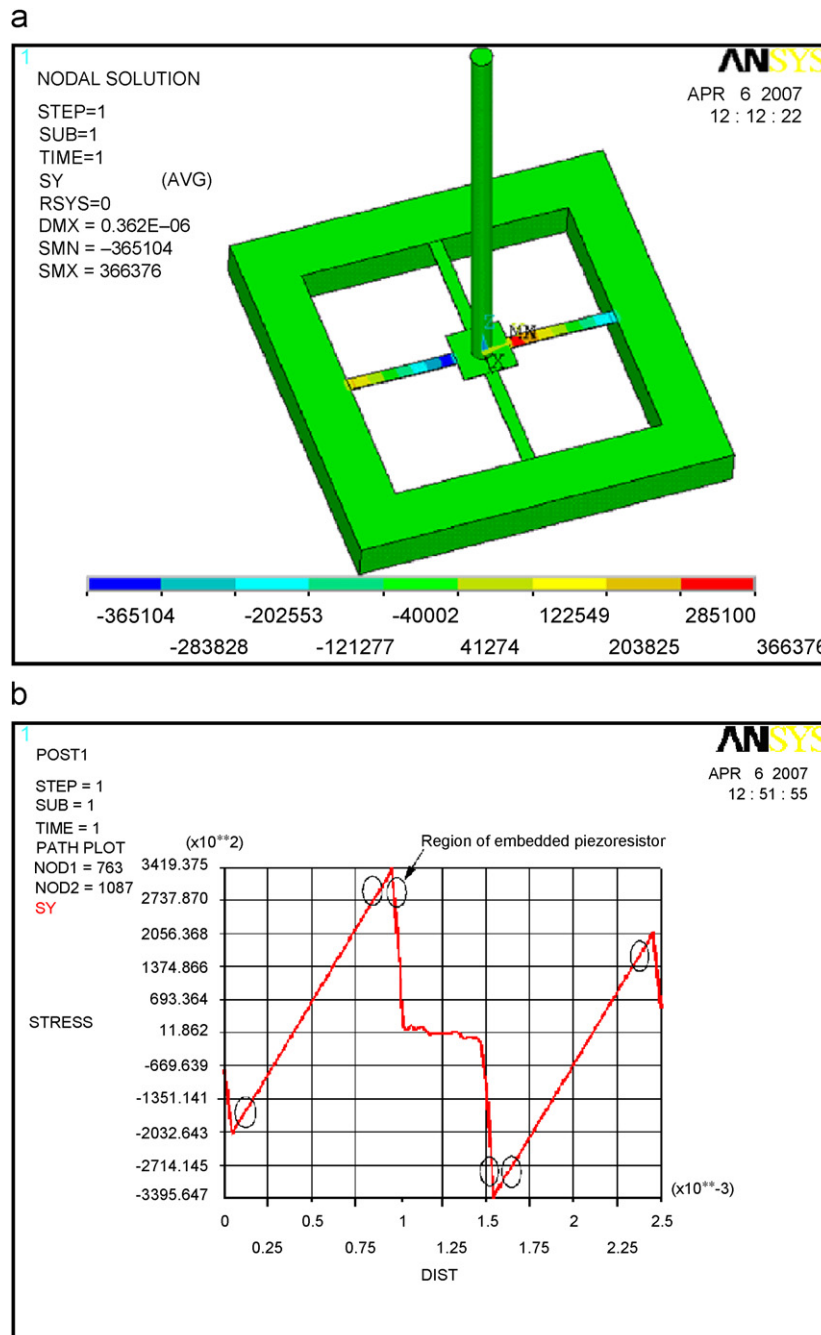


Fig. 4. (a) Schematic view and (b) curve of stress distribution on the microstructure.

stimulating the hair cell. Therefore, the bionic structure mainly includes the design of hair cell and its stereocilia. In this paper, the piezoresistor is simulated to hair cell and the rigid plastic cylinder is simulated to stereocilia.

The structure of hydrophone consists of two parts: four-beam microstructure and rigid plastic cylinder which has the same density as that of water. Fig. 3 shows the actual design of this structure. Fig. 3(a) is the three-dimensional (3D) model of the design and Fig. 3(b) gives the two-dimensional (2D) top view of the design. The four-beam microstructure consists of four vertical cantilever beams. The rigid plastic cylinder is fixed at the center block of the four-beam microstructure. Both the center block and the beams have the same thickness. The whole structure has complete axial symmetry in the xoz plane and $yo z$ planes.

According to acoustics theory, only when the cylinder and the surrounding medium have the same density can the cylinder and the medium particle have synchronous vibration, or else the acoustic information cannot be exactly memorized. In this paper, the rigid plastic cylinder not only has the same density as that of water but also has small geometric size (diameter: $200\ \mu\text{m}$, length: $5000\ \mu\text{m}$), meeting the vibration conditions well.

When the plastic cylinder responds directly to the acoustic particle motion, the center block will have a horizontal displacement and an angular rotation. Therefore, the structure will be subject to deformation, an amplified and concentrated strain is generated on the slim sensing beams. A full-active Wheatstone bridge is logically formed by locating eight piezoresistors which is used to sense the deformation of the beams. This bridge structure can increase the hydrophone's sensitivity by about two orders of magnitude without sacrificing the natural frequency of the hydrophone. The resistance of the

piezoresistor implanted into sensitive structure is changed when the signal is transmitted to it. When there is incentive direct current, the bridge's change will be detected. Therefore, the vector underwater acoustic signal will be detected also.

Considering the present fabrication technology, the center block of the modeled structure element is $500\ \mu\text{m}$

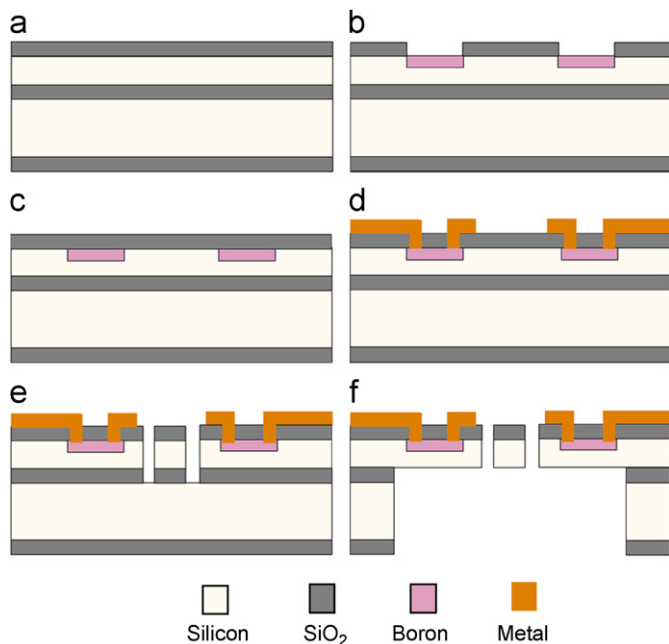


Fig. 5. (a)–(f) Fabrication sequence of the microstructure.

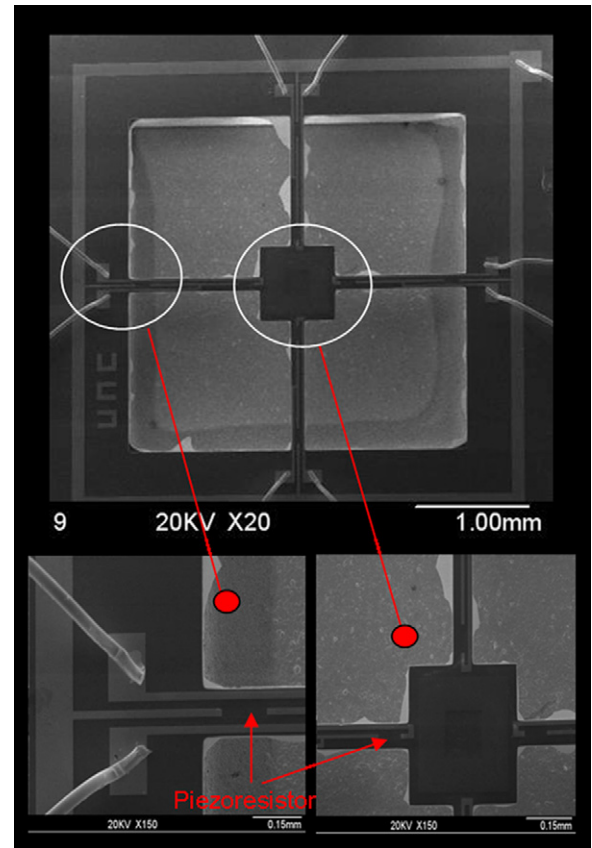


Fig. 6. SEM images (top view) of the microstructure.

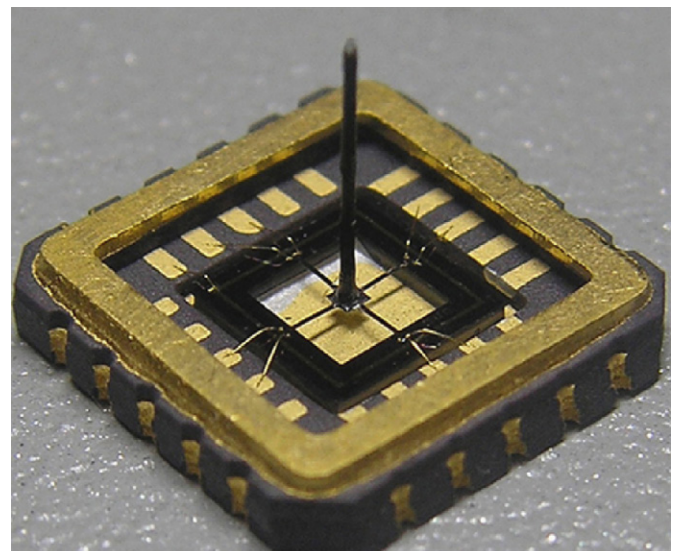


Fig. 7. Photo of the hydrophone structure.

long, 500 μm wide, and 10 μm thick. The four beams are 1000 μm long, 120 μm wide, and 10 μm thick.

To verify the accuracy of the above model and evaluate its performance, the static behavior of the hydrophone's structure is studied by means of finite element modeling (FEM) in this section. We used 45 solid, 3D elements. All the elements are standard cuboids; the ratio among length, width, and height is close to 1:1:1. Fig. 4(a) shows the distribution of simulated stress on a beam under static excitation. As expected, the maximal stress is located at the edge of the beam–block interface and near the support frame. The piezoresistors of the structure can be located at these places of the beam where the stress profile is optimal (single sign and uniform distribution, as shown in Fig. 4(b)).

4. Fabrication

The fabrication of the hydrophone consists of the processing of four-beam microstructure and the manufacture of rigid plastic cylinder. The rigid plastic cylinder can be easily achieved by plastic molding processing. The four-beam microstructure is manufactured by means of the silicon-on-insulator (SOI) wafer with MEMS technology. The fabrication procedures are illustrated in Fig. 5.

The SOI wafer has a 10 μm device layer. The buried oxide layer is 2 μm thick, with a 400 μm thick handle wafer (substrate). An additional thermal SiO_2 layer, 2 μm thick, is present on the backside of the handle wafer. A PECVD SiO_2 layer has been deposited on the device layer to act as a mask for the implantation step (Fig. 5(a)). The implantation windows have been photolithographically patterned and the PECVD SiO_2 has been subsequently etched. When the etch is complete, the photoresist has been removed and boron has been implanted (Fig. 5(b)). In the activation process of implanted boron, the anneal temperature has been 1000 $^\circ\text{C}$ and the anneal duration has been 35 min. Then, a 255 nm thick PECVD SiO_2 passivation layer has been deposited on the wafer (Fig. 5(c)).

To define the metal tracks, the windows of the metal to silicon contacts have been opened using the same process as the implantation windows to reveal the underlying p-type doped silicon. After the resist has been stripped in a fuming nitric acid solution, an aluminum–1% silicon metal layer has been deposited on the wafers. The metal layer has been patterned by photolithography and etched to define the metal tracks (Fig. 5(d)). The cantilevers in the device layer have been etched in an inductively coupled plasma (ICP) reactor after the SiO_2 passivation layer has been removed and the 2 μm thick buried oxide has been subsequently removed (Fig. 5(e)). In the last step, the wafer has been aligned on the backside and the structures have been released by ICP process, and then the buried oxide layer has been removed by a dry etch step as shown in Fig. 5(f). The SEM image (top view) of the microstructure is shown in Fig. 6.

5. Packing and measurement

After the four-beam microstructure is fabricated, a rigid plastic cylinder is fixed at the center of the microstructure as shown in Fig. 7, then packaged in a hat which is made of sound-transparent polychloroprene rubber. A built-in high-quality, lownoise, 50 dB preamplifier provides signal conditioning for transmission over long underwater cables. An integrated waterproof rubber ring allows quick disconnection of the cable and makes replacements and storage very easy. In order to make the motion of the rigid plastic cylinder be the same as that of the acoustic medium particle, castor oil that has the same density as that of water is poured into the hat and low-noise cable is led out.

Special care has been taken in the production of the cable in order to obtain good electrical shielding. This also enables the hydrophones to avoid high electromagnetic interference. The support body of the hydrophones is made of aluminum–bronze alloy which has extremely high corrosion resistance in virtually all hostile environments, and very good anti-fouling properties when immersed in seawater (Fig. 8).

The measurement of the hydrophone was processed in a pool of first-class national-defense underwater acoustic calibration station. These were measured in free-field conditions achieved by means of pulse techniques. This method requires a standard hydrophone as a projector and the fabrication hydrophone as the receiver. An example of the transmitted waveform and the received waveform of the hydrophone is shown in Fig. 9, and the receiving sensitivity of the hydrophone is -197.7dB

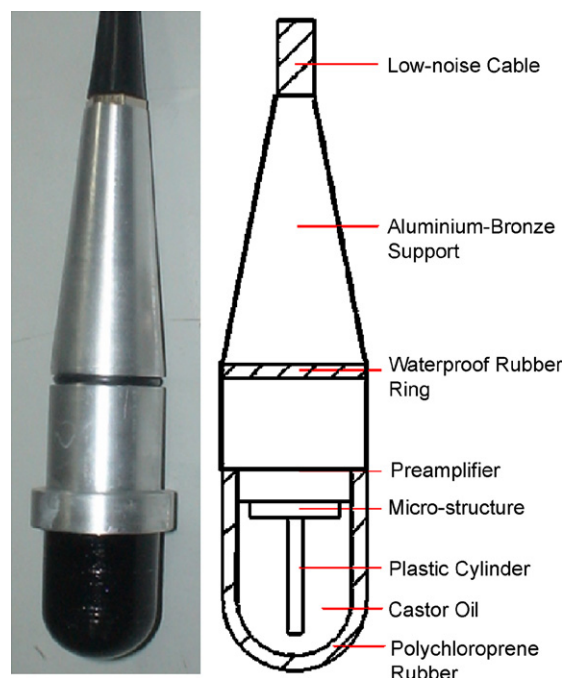


Fig. 8. Photo of packaged hydrophone.

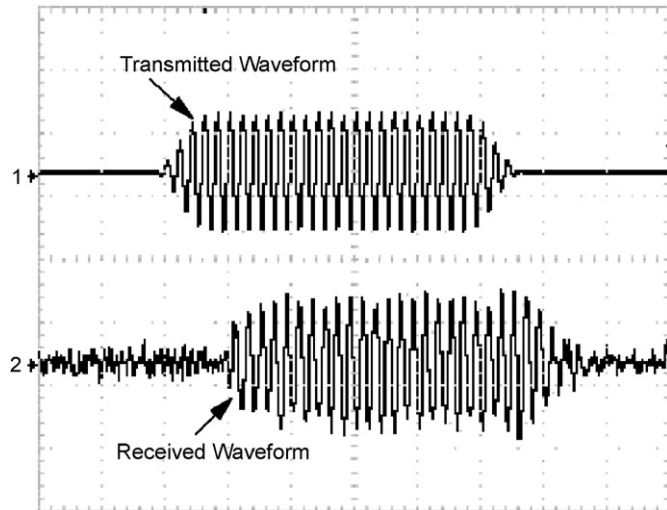


Fig. 9. Examples of transmitted and received waveforms.

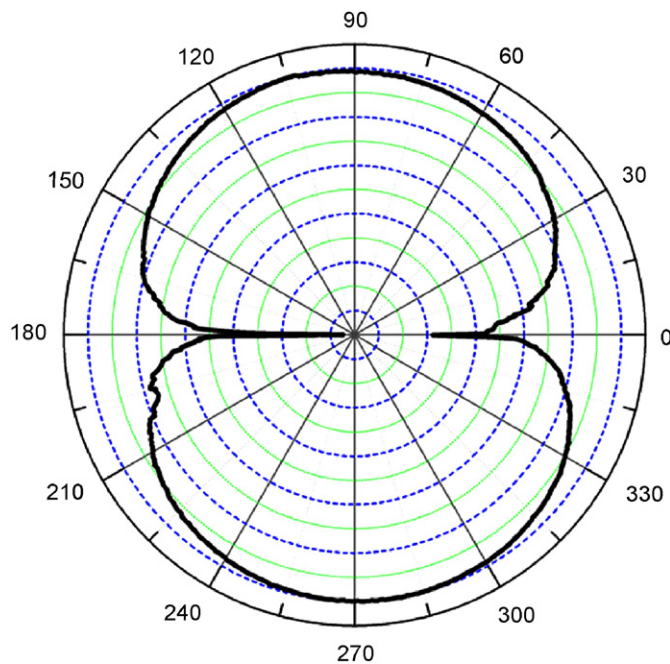


Fig. 10. Directivity patterns of the hydrophone.

($0\text{ dB} = 1\text{ V}/\mu\text{Pa}$). The directivity patterns of the hydrophone have been found with software for the turntable at the frequency of 40 Hz (Fig. 10).

The test results show that the novel MEMS vector hydrophone possesses directional pattern in the form of “8” shape and the resolution of the directivity pattern $K_d > 20\text{ dB}$.

6. Conclusion

The design, simulation, fabrication, and preliminary characterization of the novel MEMS bionic vector hydrophone have been presented. As expected, this hydrophone is more miniature compared with the traditional hydrophone by means of the ingenious bionic structure and MEMS technology, and the low-frequency characteristic of the hydrophone is desirable because of the application of piezoresistive effect. It possesses good directional pattern in the form of “8” shape, and the receiving sensitivity of the hydrophone is up to -197.7 dB ($0\text{ dB} = 1\text{ V}/\mu\text{Pa}$).

At present, initial design and experiments have been performed. How to improve the sensitivity of the hydrophone and expand its available band will be the future work.

Acknowledgements

This work has been financially supported by the National Natural Science foundation of China (Grant No. 50405025, 50535030) and Program for New Century Excellent Talents in University (NCET) of China.

References

- [1] F. Shi, P. Ramesh, S. Mukherjee, *Comput. Struct.* 56 (1995) 769–783.
- [2] B. Bhushan, *Microelectron. Eng.* 84 (2007) 387–412.
- [3] T. Thundat, L. Maya, *Surf. Sci.* 430 (1999) 546–552.
- [4] M. Gad-El-Hak, *The MEMS Handbook*, CRC, New York, 2002.
- [5] P. Passian, G. Evans, V.K. Varma, *Rev. Sci. Instrum.* 74 (2003) 1031–1035.
- [6] P. Gruber, B. Imhof, *Acta Astronaut.* 60 (2007) 561–570.
- [7] H.M. Muller, *Comp. Biochem. Physiol.* 114A (1996) 257–263.
- [8] S. Jande, *J. Ultrast. Res.* 15 (1966) 496–509.
- [9] W.K. Metcalfe, C.B. Kimmel, E. Schabtach, *J. Comp. Neurol.* 233 (1985) 377–389.
- [10] R.E. Newnham, in: *Proceedings of the IEEE Frequency Control Symposium, 1992*, pp. 513–524.
- [11] K. Kim, T.B. Gabrielson, G.C. Lauchle, *J. Acoust. Soc. Am.* 116 (1991) 3384–3392.
- [12] B.A. Moffett Mark, *J. Acoust. Soc. Am.* 45 (1998) 1346–1351.
- [13] C.B. Leslie, J.M. Kendall, J.-L. Jones, *J. Acoust. Soc. Am.* 28 (1956).